acta physica slovaca vol. 46 No. 1, 41 – 56 February 1996

EFFECT OF DEFORMED TARGET NUCLEUS ON ELASTIC SCATTERING REACTIONS

M.Y.M. Hassan, Z. Metawei[1]
Physics Department, Faculty of Science, Cairo University, Giza, Egypt

Received 4 April 1995, in final form 22 August 1995, accepted 20 December 1995

The elastic scattering differential cross-section and the reaction cross-section are calculated for ^{12}C - ^{12}C ($E/A \approx 85$ MeV), ^{16}O - ^{12}C ($E/A \approx 94$ MeV) and α - ^{12}C ($E/A \approx 342.5$ MeV). The high-energy double-folding optical potential approximation to the exact nucleus-nucleus multiple scattering series derived by Wilson is used. The Pauli correlation effect is considered. This folding approach is applied to spherical and deformed target nuclei. The projectile is considered to be spherical in the two cases. Introducing the Pauli correlation effect improves the agreement at large angles. Considering the target as a deformed nucleus leads to the best agreement.

1. Introduction

In the last few years a large amount of experimental data has become available in the field of heavy-ion grazing collisions at intermediate energies, such as elastic and inelastic scattering, stripping and pickup reactions, and spin and isospin exchange.

The study of the elastic scattering is the simplest approach to test the nucleus-nucleus interaction. The optical model potential between two nuclei serves as a basic theoretical tool in describing elastic scattering as well as more complicated reactions. The most famous methods for calculating the optical potential are the phenomenological Woods-Saxon, the proximity, the semiclassical, the model independent, the self consistent, the energy density and the double folding model.

At very high energy, a general multiple scattering theory of composite particle has been developed by Wilson [1], in which the transition amplitude is derived in terms of sequences of two body scattering and free peojectile-target propagator. The series reduces to the usual Watson's [2] multiple scattering series when the projectile is elementary. Wilson and Townsend [3] used the multiple scattering series to derive the approximate optical model scattering series. The double folding potential is obtained by folding the energy dependent free nucleon-nucleon interaction with the densities for both projectile and target. Townsend et al. [4] generalized the model to include the Pauli correlation

[1]E-mail address: m zeinab@frcu.eun.eg

effects in order to investigate the geometrical nature of high energy nucleus-nucleus reaction cross-section. They found that the Pauli exchange correlation effects are unimportant when determining the total and absorption cross-sections. Bidasaria et al. [5] calculated the elastic scattering, the reaction and the total cross-sections for ^{12}C - ^{12}C at energies from 200 to 290 MeV. They used the optical potential derived by Wilson in the context of the eikonal phase shift. The minor disagreement between theory and experiment was attributed to uncertainties in the real part of the forward neutron-proton scattering amplitude. The remaining discrepancies were attributed to the negligence of the Fermi motion, the off shell effects and the Pauli correlations. However, limiting the experimental slope parameter values to those appropriate to diffractive scattering has improved the agreement between the theoretical calculation and the experimental data for ^{12}C - ^{12}C elastic scattering in the energy range 200 - 300 MeV [6]. This showed the validity of the eikonal expansion at this low energy. Owing to the simplicity of this model, it is clearly worth assessing the applicability of this method to intermediate energy heavy ion scattering processes. Also, in this method the nucleus - nucleus collision could be described by means of the same underlying theoretical framework. So, it could be tested in a wide variety of collisions.

It is well established that in many cases, such as nuclear rainbow scattering, observed for α - particles and some light heavy ion or the elastic scattering data for ^{16}O and ^{12}C at intermediate energies [7], where the data are sensitive to the real optical potential over a wider radial domain, the folding model failed to give a good description to the data. Therefore, some modifications of the folding model have been made to eliminate such a deficiency of the folded potentials. One of these approaches is to impose on the widely used M3Y effective NN interaction an explicit density dependence, the DDM3Y interaction. Another is to treat correctly the single nucleon knock - on exchange effects arising from the Pauli principle. Also, the coupling to the collective states could improve the theoretical calculations using the folding model to fit the experimental data. Ohtsuka [7] showed that the correct treatment of the exchange potential leads to a more realistic shape of the real optical potential calculated for ^{16}O and ^{12}C scattering data at intermediate energies. ^{12}C - ^{12}C and ^{16}O - ^{12}C reactions were investigated by Brandan and Satchler [8] using a double folded potential based on the density and energy dependent DDM3Y interaction. It is well known that the origin of the density dependence of the effective interaction comes mainly from the Pauli principle effect in the overlapping region and from the energy denominator of the Bethe - Goldstone equation [9]. In these calculations [8] a normalization factor to the real potential was used to obtain the fit with experimental data.

Kobos et al. [10] verified that the coupling to the 2^+ state of ^{12}C could be reproduced quite accurately by a small change ($\approx 5\%$) in the strength of the absorptive potential. ^{12}C - ^{12}C at $E/A \approx 85$ MeV was investigated using the complex reaction matrix [11] - [13]. The coupling to the 2^+ and 3^- collective states were included in these calculations, which gave a good agreement with the experimental data. They obtained a negative sign for the deformation parameter B_{20}, which reflects the fact that ^{12}C nucleus has an oblate shape and this was favoured by their calculations over a positive sign. Faessler et al. [13] have investigated the same reaction in the energy density formalism and

including the coupling to the collective states. The comparison of these results with the experimental data showed that the inhancement of the imaginary part in the optical potential improves the agreement with experimental data, whereas the repulsive contribution to the real part is unfavourable to explain the experimental cross-section. This reaction was analyzed [14] in the optical and Glauber models. This analysis showed that the reaction cross-section in ion-ion scattering in this intermediate energy region is much smaller than that at lower energies. Consequently, the ion makes a much closer approach than that at lower energies, which means that the elastic scattering measurements at 85 MeV/n allow to determine the ion-ion potential down to a much smaller inter-nuclei distance than at low incident energies, this has been confirmed later for the ^{16}O - ^{12}C system at 93 MeV/n [15]. This shows that at this intermediate energy the nuclei increase the overlapping and Pauli correlations become important. Since, it was found that [16], when the Pauli principle was considered, the potential turns out to be more repulsive. This effect could be further traced to the increase in kinetic energy of the separate nucleons that take place when the bombarding energy is low enough to cause overlapping of the Fermi spheres associated with each ion. $\alpha-^{12}C$ system at 1370 MeV was investigated using Glauber theory [17], [18] and the effects of nuclear correlations were considered, also the coupling to the collective states of ^{12}C - nucleus [17] was considered. Good agreement with experimental data was obtained for small scattering angles.

Our interest in this work is to test the validity of the optical potential derived by Wilson in the context of the eikonal approximation to calculate the elastic scattering differential cross-section and the reaction cross-section at intermediate energies. Also, we would like to test the effect of introducing the Pauli correlation effect and considering the target nucleus as a deformed nucleus on the calculations of the elastic scattering reactions.

In section II we describe our formalism, in which the nucleus-nucleus optical potential is introduced with and without the Pauli correlation effect. The deformation of the target nucleus is presented. And finally the density distributions considered in this work are given. Section III gives our results for the optical potential calculated with and without the Pauli correlation effect for ^{12}C - ^{12}C, ^{16}O - ^{12}C and $\alpha-^{12}C$. Our results are compared with the phenomenological optical potential. Then, the elastic scattering differential cross-section are presented and compared with the experimental data for ^{12}C - ^{12}C, ^{16}O - ^{12}C and $\alpha-^{12}C$. The effect of the Pauli exchange correlation function and considering the target as a deformed nucleus are studied. Then, the results of the reaction cross-section are presented and compared with other theoretical and experimental results for ^{12}C - ^{12}C. Finally, the conclusion is given.

2. The Formalism

2.1. The Optical Potential Model Including Pauli Correlation Effect

The nucleus-nucleus optical potential may be written as [3]

$$V_{opt}(X) = A_P A_T \int d^3r_T \rho_T(r_T) \int d^3y \rho_P(x+y+r_T) t(e,y) \qquad (2.1)$$

where A_P, A_T are the mass numbers of the projectile and the target, respectively. ρ_P and ρ_T represent the projectile and target single particle densities. $t(e,y)$ is the two body transition amplitude averaged over the constituent particles, e is the nucleon energy in the two body center of mass frame and y is the two nucleon separation distance. $t(e,y)$ has been derived from the Fourier transform of the two body scattering amplitude [19]. We use the usual parametrization of the two body scattering amplitude:

$$f(e,q) = \frac{K_N \sigma}{4\pi}(\alpha + i)\exp(-Bq^2/2) \tag{2.2}$$

This form of the scattering amplitude yields

$$t(e,y) = -(e/m)^{1/2}\sigma(\alpha + i)(2\pi B)^{-3/2}\exp(-y^2/2B) \tag{2.3}$$

where q is the momentum transfer, K_N is the wave number of the incident nucleon, m is the nucleon mass, σ is the average nucleon-nucleon (NN) total cross-section, α is the average of the ratio of the real to the imaginary parts of the NN forward scattering amplitude and B is the slope parameter of the NN elastic scattering differential cross-section.

Equation (2.1) does not include the correlation effects due to Pauli exclusion principle. Considering correlation due to Pauli principle, equation (2.1) may be written as [20]

$$V_{opt}(X) = A_P A_T \int \mathrm{d}^3 r_T \rho_T(r_T) \int \mathrm{d}^3 y \rho_P(x + y + r_T) t(e,y)[1 - C(y)] \tag{2.4}$$

where the Pauli correlation function in the Fermi gas model is given by [20]

$$C(y) \approx \frac{1}{4}\exp(-K_F^2 y^2/10) \tag{2.5}$$

with

$$K_F = 1.36 \quad \mathrm{fm}^{-1}.$$

2.2. The Elastic Scattering Differential Cross-Section

The elastic scattering differential cross-section for symmetric system (^{12}C - ^{12}C) is given by

$$\sigma_{el}(\Theta) = |f(\Theta) + f(\pi - \Theta)|^2 \tag{2.6}$$

while for non-symmetric systems (^{16}O - ^{12}C and α-^{12}C) it is given by

$$\sigma_{el}(\Theta) = |f(\Theta)|^2 \tag{2.7}$$

The elastic scattering amplitude considering the Coulomb effect is given by

$$f(\Theta) = f_C(\Theta) + (2ik)^{-1}\sum_L (2L+1)\exp(2i\eta_L)(S_L - 1)P_L(\cos\Theta), \tag{2.8}$$

$f_C(\Theta)$ is the usual point charge Coulomb amplitude, η_L is the point charge Coulomb scattering phase shifts and S_L is given by

$$S_L = \exp(2i\delta_L) \tag{2.9}$$

where δ_L is the complex nuclear phase shift. Considering the correspondence between the quantal expression and the eikonal approximation, the reaction sross-section is determined from:

$$\sigma_R = \int \mathrm{d}^2 b[1 - T(b)] \tag{2.10}$$

where $T(b)$ is given by [21]

$$T(b) = \exp(-2\mathrm{Im}\chi(b)) \tag{2.11}$$

with

$$\chi(b) = \frac{-1}{2K}\int_{-\infty}^{+\infty} U(b,Z)\mathrm{d}Z, \tag{2.12}$$

$$U(b,Z) = [2mA_P A_T(A_P + A_T)^{-1}]V_{opt}(b,Z) \tag{2.13}$$

and K is the incident wave number.

Comparison of relation (2.10) with the usual quantal relation:

$$\sigma_R = \frac{\pi}{K^2}\sum_L^{\infty}(2L+1)(1 - |S_L|^2) \tag{2.14}$$

with

$$Kb = L + \frac{1}{2} \tag{2.15}$$

we get

$$|S_L|^2 = T(b) \tag{2.16}$$

From this, the complex nuclear phase shift is obtained from

$$\delta_L = \frac{1}{2}\chi(b) \tag{2.17}$$

In case of heavy ion collisions there is a strong Coulomb field, which causes a distortion to the original trajectory, especially at energies not exceeding 100 MeV per nucleon. For the Coulomb distortion of the trajectory, L can be related to b by the relation [22]

$$Kb = \eta + [\eta^2 + (L + \tfrac{1}{2})^2]^{\frac{1}{2}} \tag{2.18}$$

where η is the Sommerfeld parameter,

$$\eta = Z_P Z_T e^2/\hbar v.$$

2.3. The Target Deformation

The scattering of a spherical projectile nucleus from a deformed target nucleus will be studied. The density of a nucleus with an axially symmetric deformation may be written as [23]

$$\rho_T = \rho_{0T}(r) - r\frac{\mathrm{d}\rho_{0T}(r)}{\mathrm{d}r}\sum_L B_{L0}^{\rho_T} Y_{L0}(\Theta,\Phi) \tag{2.19}$$

where $\rho_{0T}(r)$ parametrizes the spherical part of the target density distribution and $B_{L0}^{\rho_T}$ is the deformation parameter of the target nuclear matter distribution. The quadrupole deformation is considered only, therefore the value of L is restricted to 2.

To calculate the deformation parameter B_{20} let us consider the transition density

$$\rho_{tr}(r) = B_{L0}^{\rho_T} r^{L-1}\frac{\mathrm{d}\rho_{0T}(r)}{\mathrm{d}r} \tag{2.20}$$

and for $L = 2$,

$$\rho_{tr}(r) = B_{20}^{\rho_T} r\frac{\mathrm{d}\rho_{0T}(r)}{\mathrm{d}r}. \tag{2.21}$$

The normalization constant $B_{20}^{\rho_T}$ is determined by assuming that the proton transition density is (Z_T/A_T) times the mass transition density and choosing B_{20} to give the measured value of $B(E2)$ for the target nucleus [24], i.e.

$$\int A_T\rho_{tr}(r)r^{L+2}\mathrm{d}r = (A_T/Z_T e)[B(EL)]^{1/2} \tag{2.22}$$

where A_T and Z_T are the mass number and the charge number of the target nucleus, respectively.

2.4. The Density Parameters

In our calculations we used nuclear single particle matter densities which are extracted from the charge density. Two forms of the charge densities are used:

a) A harmonic oscillator charge density.
b) A Gaussian charge density.

a) A harmonic oscillator charge density.

The harmonic well charge density has the form [25]

$$\rho_C(r) = \rho_0[1+\nu(r/a)^2]\exp(-r^2/a^2) \tag{2.23}$$

The constants a and ν are fitting parameters to electron scattering data [25] and ρ_0 is determined by the normalization condition

$$\int \rho(r)\mathrm{d}r = 1 \tag{2.24}$$

E_{lab} (MeV)	σ_{pp} (mb)	α_{pp}	b_{pp-2} (GeV/C)	σ_{pn} (mb)	α_{pn}	b_{pn-2} (GeV/C)	ref.
100	33.2	1.87	16.951	72.7	1	9.246	34
344	34.0	0.60	0.44	27.0	0	2	35

Table 1. The parameters of the NN amplitude that are used in the calculations reported here.

The matter density is extracted from the charge density by the method discussed in ref. (20), which gives for the harmonic well matter density

$$\rho_m(r) = \frac{\rho_0 a^3}{8S^3}\left(1+\frac{3\nu}{2}-\frac{3\nu a^2}{8S^2}+\frac{\nu a^2 r^2}{16S^4}\right)\exp(-r^2/4S^2) \tag{2.25}$$

with

$$S^2 = \frac{a^2}{4}-\frac{r_P^2}{6}$$

where ρ_P is the proton rms radius and is equal to 0.87 fm.

b) A one term Gaussian density.

The Gaussian density has the form

$$\rho_C(r) = \rho_0\exp(-r^2/a^2) \tag{2.26}$$

where

$$\rho_0 = 1/(a\sqrt{\pi})^3 \tag{2.27}$$

and

$$a = \langle r^2\rangle^{1/2}(1.5)^{-1/2} \tag{2.28}$$

The corresponding matter density is

$$\rho_m(r) = \frac{\rho_0 a^3}{8S^3}\exp(-r^2/4S^2)$$

with

$$S^2 = \frac{a^2}{4}-\frac{r_p^2}{6}$$

3. Results and Discussion

In this section we present our results for the elastic scattering of ^{12}C - ^{12}C, ^{16}O - ^{12}C and α–^{12}C at energies 1016 Mev, 1503 MeV and 1370 Mev, respectively. ^{12}C and ^{16}O are described by harmonic oscillator charge density. For α–^{12}C reaction, a one term Gaussian matter density is considered for α-particle and harmonic oscillator matter density for ^{12}C nucleus. The parameters for nucleon-nucleon scattering amplitude which are used in this calculations are listed in table (1).

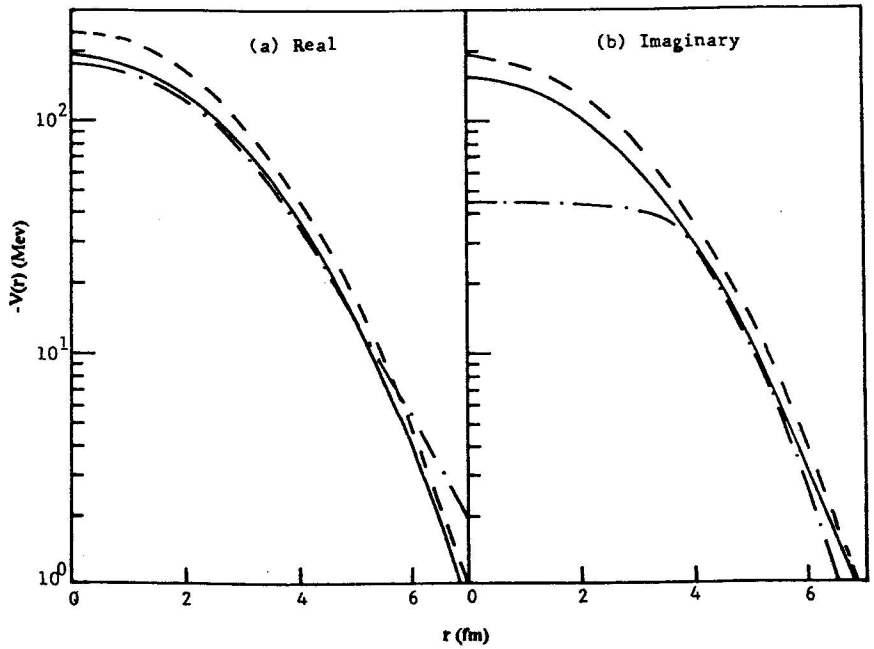

Fig. 1. The real (a) and the imaginary (b) parts of the optical potential for ^{12}C - ^{12}C elastic scattering at 1016 MeV (dashed line), compared with phenomenological potential (dashed dotted line). The solid line represents the calculations including the Pauli correlation effect.

Reaction	V (MeV)	r_r (fm)	a_r (fm)	W (MeV)	r_i (fm)	a_i (fm)	ref.
^{12}C - ^{12}C	200	0.550	0.980	43.11	0.990	0.530	28
^{16}O - ^{12}C	120	0.748	0.893	27.40	1.050	0.723	15
α - ^{12}C	65.58	0.733	0.683	229.8	0.733	0.683	36

Table 2. The phenomenological optical potential parameters.

3.1. The Optical Potential Calculations

The real and the imaginary parts of the optical potential for ^{12}C - ^{12}C at 1016 MeV with and without Pauli correlation effect are shown in Fig. 1. The same calculations for ^{16}O - ^{12}C and α - ^{12}C are shown in Fig. 2. and 3., respectively. Our calculations of the optical potential are compared with the phenomenological potential whose parameters are given in Tab. 2. We can notice from Fig 1.-3. that, introducing the Pauli correlation effect for the three reactions, improves the agreement with the phenomenological

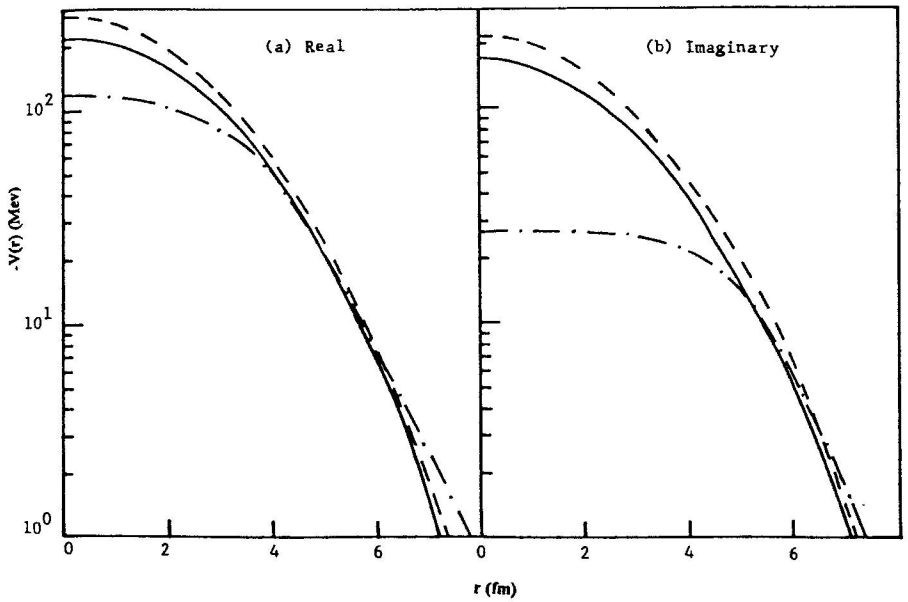

Fig. 2. The same at Fig. 1. but for ^{16}O - ^{12}C at 1503 MeV.

Reaction	(a)			(b)		
	$b_{1/2}$ [fm]	L_g $\hbar$	R_{sa} [fm]	$b_{1/2}$ [fm]	L_g	R_{sa} [fm]
^{12}C - ^{12}C	5.6	67	5.65	5.8	69.5	5.85
^{16}O - ^{12}C	6.1	88	6.15	6.2	90.0	6.25
α - ^{12}C	3.5	42	3.51	3.6	43.0	3.61

Table 3. The strong absorption parameters: (a) $C(y) \neq 0$ and (b) $C(y) = 0$.

potential. Also, we can see that the potential becomes shallower by introducing Pauli correlation correction. This was justified before by Hernandez and Moszkowski [16]. Comparing the potential obtained for ^{12}C - ^{12}C with that obtained for ^{16}O - ^{12}C, we find that the real part of ^{16}O - ^{12}C optical potential is more attractive and its imaginary part is more absorptive.

The strong absorption radius is calculated for the three reactions using the transparency function, $T(b)$ [21]. A typical representation of $T(b)$ is shown in Fig. 4. for ^{12}C - ^{12}C reaction. We can notice from Fig. 4. that the lower partial waves are totally absorbed. The $T(b)$ distribution can be used to define the strong absorption radius, R_{sa}, a quantity which characterized the system with respect to the strong absorption. R_{sa} is the distance of the closest approach on the Coulomb trajectory associated with the grazing partial wave L_g for which $T(b) = 1/2$.

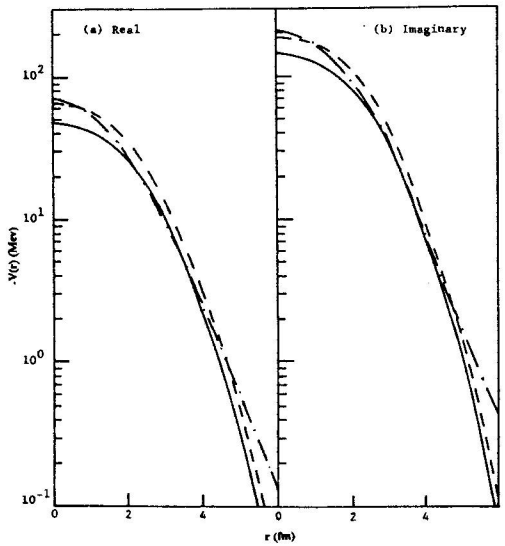

Fig. 3. The same as Fig. 1. but for α - ^{12}C at 1370 Mev.

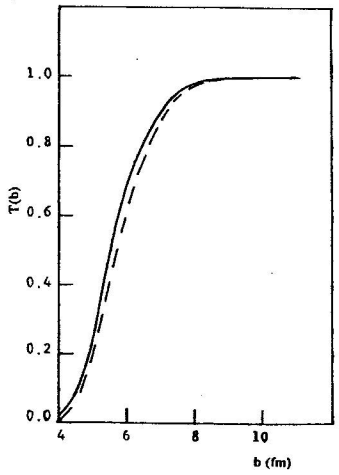

Fig. 4. The transparency function T(b) calculated for ^{12}C - ^{12}C system at $E/A \approx 85$ MeV. Solid line: C(y) considered. Dashed line: C(y) neglected.

The strong absorption impact parameter $b_{1/2}$, for which $T(b) = 1/2$ defines the grazing partial waves L_g as [26]

$$Kb_{1/2} = L_g + \frac{1}{2} \tag{3.1}$$

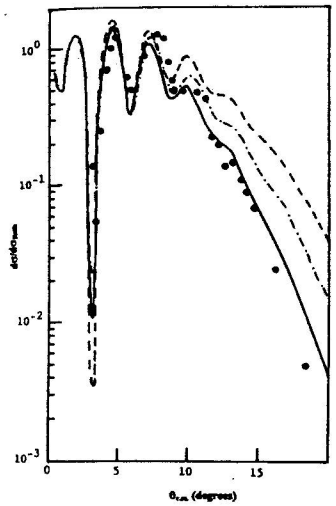

Fig. 5.

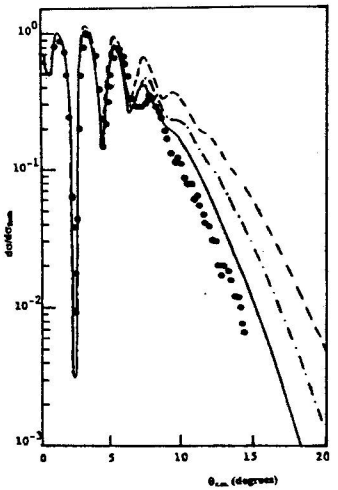

Fig. 6.

Fig. 5. The elastic scattering differential cross-section for ^{12}C - ^{12}C system at $E/A \approx 85$ MeV (dashed line). Dashed dotted line represents the inclusion of Pauli correlation effect. Solid line represents the calculations considering Pauli correlation effect and the deformation of the target nucleus.

Fig. 6. The same at Fig. 5. but for ^{16}O - ^{12}C system at $E/A \approx 94$ MeV.

Reaction	$\lvert V\rvert/E$	
	C(y)=0	C(y)≠0
^{12}C - ^{12}C	0.240	0.190
^{16}O - ^{12}C	0.180	0.146
α - ^{12}C	0.047	0.035

Table 4. The ratio $|V|/E$ for all reactions considering C(y) and neglecting it.

Hence the strong absorption radius can be calculated from:

$$R_{sa} = \left(\eta + \left[\eta^2 + \left(L_g + \frac{1}{2}\right)^2\right]^{1/2}\right) \; / \; K \tag{3.2}$$

where η is the Sommerfeld parameter. The values of $b_{1/2}$, L_g and R_{sa} for all the reactions considered are given in Tab. (3 a,b) with and without Pauli correlation, respectively. From these tables, we can see that by introducing the Pauli correlation effect, the strong absorption radius decreases slightly.

From figures (1 - 3) and tables (3 a,b) we can see that our potentials have nearly the same values as the phenomenological potentials at the strong absorption radius.

Reaction	Present calculations								Other results [21]				Experim. data
	C(y)=0			C(y)≠0			σ_R mb						
	$b_{1/2}$ fm	$\sigma_R = *b_{\frac{1}{2}}^2$ mb	σ_R mb	$b_{1/2}$ fm	$\sigma_R = *b_{\frac{1}{2}}^2$ mb	σ_R mb	C(y)≠0 $B_{20} \neq 0$		$b_{1/2}$ fm	$\sigma_R = *b_{\frac{1}{2}}^2$ mb	σ_R mb		σ_R mb
^{12}C - ^{12}C	5.8	1057	1086	5.6	985	1032	1119		5.5	950	988		996^{+50}_{-250} [28]
^{16}O - ^{12}C	6.2	1208	1244	6.1	1169	1186	1280						960 ± 25 [37] (1000) [35]
α - ^{12}C	3.6	407	442	3.5	385	400	445						(1380) [8] 450 ± 20 [38]

Table 5. The nucleus-nucleus reaction cross section compared with other calculated results [21] and with experimental results [28], the experimental result in paranthesis was extracted from optical model analysis. The experimental nucleus-nucleus σ_R was extracted from the optical model analysis [8], [21] (in parentheses) and the rest from direct measurements [28], [37].

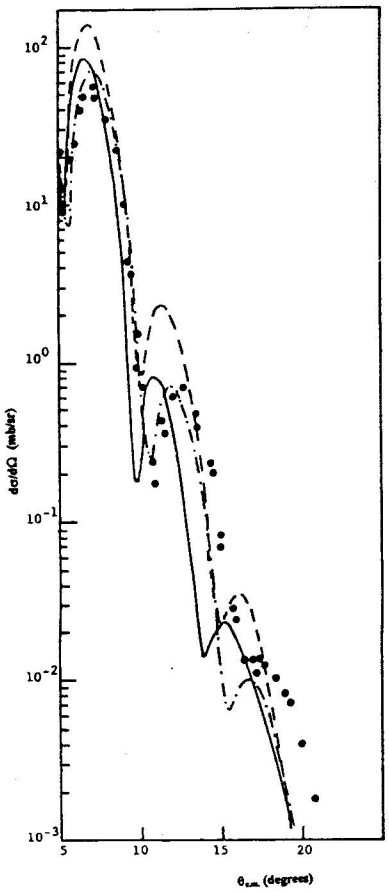

Fig. 7. The same at Fig. 5. but for α - ^{12}C system at 1370 MeV.

The optical potential is used to calculate the elastic scattering differential cross-section. The condition for applying the eikonal approximation is contained in the relation [26]

$$|V|/E \ll 1 \tag{3.3}$$

This ratio is calculated for the potentials shown in figures (1 - 3) and is listed in table (4). We can see that the condition (3) is justified for all cases considered.

3.2. The Effect of the Pauli Correlation and the Deformation of the Target Nucleus on the Elastic Scattering Differential Cross-section

The elastic scattering differential cross-section is calculated for all the above reactions with and without the Pauli correlation effect. Also, it is calculated taking into account the Pauli correlation effect together with the deformation of the target nucleus. The choice of $B(E2) = 42e^2$ fm^4 for ^{12}C nucleus [24], [27] yields a deformation parameter $B_{20} = \pm 0.447545$. We found that the negative sign of the deformation parameter leads to a better agreement with experimental data than the positive sign, which was confirmed by Faessler [12]. So, we used the negative sign of the deformation parameter in our calculations. All our theoretical results are compared with experimental data [15], [28], [29].

Figure 5. shows the elastic scattering differential cross-section for ^{12}C - ^{12}C system, calculated with and without Pauli correlation effect and considering the Pauli correlation effect together with the deformation of the target nucleus. We notice from this figure that the three types of calculations give a satisfactory agreement with experimental data up to $\Theta_{cm} \approx 9°$. Introducing Pauli correlation effect improves the agreement with the experimental data at and beyond the fourth maximum i.e. $\Theta_{cm} \geq 9°$. Reliable agreement between the theoretical and the experimental results is obtained when the Pauli correlation effect together with the deformation of the target nucleus is considered. Fig. 6. is the same as Fig. 5. but for ^{16}O - ^{12}C elastic scattering. We can see from this figure that all our calculations fairly describe the experimental data up to $\Theta_{cm} \approx 8°$. Introducting Pauli correlation effect improves the agreement with the experimental data for $\Theta_{cm} \geq 8°$. However, it gives deeper values at the first minimum. The best agreement with experimental data is obtained by taking the deformation of the target nucleus into account together with Pauli correlation effect.

We can see from the above results that three is slight disagreement at large scattering angles. It was found that for the projectiles of mass number ($A \geq 12$), the scattering processes are dominated by strong absorption effect which gives rise to strongly diffractive angular distribution [30]. This phenomenon [24] can be quantitatively expressed by the ratio of the imaginary to the real well depth of the optical potential, which is found to be about 1/3 for light projectile ($A < 12$) and larger than 1 for ^{12}C and ^{16}O. In our case this ratio is given by $1/\alpha$ It is about 0.7874 for ^{12}C - ^{12}C and ^{16}O - ^{12}C corresponding to energy per nucleon 100 MeV. However, the elastic scattering considered corresponds to energies per nucleon 85 MeV and 94 MeV, respectively, while a set of NN parameters at $E/A = 85$ MeV for ^{12}C - ^{12}C and 94 MeV for ^{16}O - ^{12}C may lead to a better agreement with the experimental data. To the best of our knowledge we did not find such a set and we used a set of $E/A = 100$ MeV.

Fig. 7. shows the elastic scattering differential cross-section for α - ^{12}C at 1370 MeV. We can see from this figure that all our calculations fairly describe the experimental data up to $\Theta_{cm} \approx 8°$. Considering Pauli correlation effect improves the agreement between theoretical and experimental data at the first and second maxima. Introducing the Pauli correlation effect together with the deformation of the target nucleus gives less satisfactory results, since the position of all the maxima and the minima are shifted towards smaller angles.

We can conclude that the high energy double folding potential derived by Wilson could describe the elastic scattering differential crossection for the three reactions considered in this work, and it could be used at intermediate energies. Introducing the Pauli correlation effect improves the agreement with the experimental data at large angles for the three reactions. Considering the deformation of the target nucleus together with the Pauli correlation effect produces the best fit to the experimental data for ^{12}C - ^{12}C and ^{16}O - ^{12}C systems. But worsen the agreement for α - ^{12}C scattering. We can also notice from Fig. 5. - 7. that the best agreement obtained at large angles for ^{12}C - ^{12}C system, where the two nuclei is of the same size.

Comparison of our results with the previous work, shows that, we attain better agreement for α - ^{12}C than that of ref. [31], especially for $\Theta > 10°$. Comparison with the same work for ^{12}C - ^{12}C and ^{16}O - ^{12}C, reveals that the overall agreement is also better. In general using the Pauli correlation effect gives much better agreement at large angles. And the calculations considering the deformation of the target nucleus, improves the agreement even better than those authors [31] who used more sophisticated density distribution.

The elastic scattering is analyzed taking into consideration the Coulomb distortion of the trajectory. The results obtained are mainly identical with the previous ones neglecting such effect. This shows that this correlation is important only in the case of scattering of heavy nuclei $\geq^{40} Ar$ [22]. This was justified by Lenzi et al. [32].

3.3. The reaction Cross-Section

The reaction cross-section is calculated for the reactions under consideration using equation (2.10), by considering the Pauli correlation effect and neglecting it. The values of the reaction cross-section are listed in Tab. 5. together with other theoretical results and compared with the experimental values which were extracted from the optical model analysis. We can see from this table that, introducing the Pauli correlation function C(y) into the calculations of the reaction cross-section gives better agreement with the experimental data than those calculated neglecting C(y) which agrees with the results of the elastic scattering.

The strong absorption impact parameter, $b_{1/2}$, provides good estimate of the reaction cross-section $\pi b^2_{1/2}$. These results are shown in Tab. 5. together with other theoretical calculations [21].

The effect of the deformation of the target nucleus on the calculated reaction cross-section is investigated and the results are shown in Tab. 5. The reaction cross-sections calculated using the negative deformation parameter give comparable results with the experimental data.

4. Conclusion

In this work the simple double - folding optical potential proposed by Wilson [3] is used to calculate the elastic scattering differential cross-section and the reaction cross-section for nucleus - nucleus reactions at different values of energies. The angular distribution of the elastic scattering shows a strong oscillatory structure at forward angles, which corresponds to Fraunhofer diffraction pattern. The oscillatory structure becomes smooth at larger angles which is one of the characteristics of nuclear rainbow scattering.

Introducing the Pauli correlation effect, the optical potential becomes shallover and have smaller values at the strong absorption radius. This gives a better agreement at large scattering angles when calculating the elastic scattering differential cross-section. Also, the Pauli correlation effect improves the agreement between the calculated reaction cross-section and the experimental data.

The elastic scattering differential cross-section calculated using negative sign for the deformation parameter gives a good agreement for the experimental data.

Our formalism considering the Pauli correlation effect and the deformation of the target nucleus gives a good agreement for the elastic scattering differential cross-section of heavy ions. However, better agreement can be attained if one takes into consideration the following points (corrections):

a) The density used for both the target and the projectile may be considered in a more sophisticated form such as a Wood - Saxon or a modified Fermi density for heavy ions.

b) The 2^+ state of the deformed target nucleus is considered in our work and the 3^- is neglected, so in future we can perform this work considering both the 2^+ and 3^- states of the deformated target nucleus.

c) The mutual excitation of the projectile and the target was observed [30] and becomes relatively stronger at large angles in the calculation of the elastic scattering. This factor is not investigated in our work, but one can consider both the target and the projectile to have excited states, i. e. both of them treated as a deformed nuclei.

d) The transition matrix element t(e,y) can be replaced by another one such as derived by Love and Franey [33].

References

[1] J.W. Wilson: *Phys. Lett.* **B52** (1974) 149
[2] K.M. Watson: *Phys. Rev.* **89** (1953) 575
[3] J.W. Wilson, L.W. Townsend: *Can. J. Phys.* **59** (1981) 1569
[4] L.W. Townsend, J.W. Wilson, H.B. Bidasaria: *Can. J. Phys.* **60** (1982) 1514
[5] H.B. Bidasaria, L.W. Townsend, J.W. Wilson: *J. Phys.* **G9** (1983) L17
[6] H.B. Bidasaria, L.W. Townsend: *Can. J. Phys.* **61** (1983) 1660
[7] Dao Tun Khoa, A. Faessler, N. Ohtsuka : *J. Phys. G: Nucl. Part. Phys.* **16** (1990) 1253
[8] M.E. Brandan, G.R. Satchler: *Nucl. Phys.* **A487** (1988) 477
[9] A.M. Kobos, B.A. Brown, P.E. Hodgson, G.R. Satchler, A. Budzanowski: *Nucl. Phys.* **A384** (1982) 65
[10] A.M. Kobos, M.E. Brandan, G.R. Satchler: *Nucl. Phys.* **A487** (1988) 457
[11] A. Faessler, W.H. Dickhoff, M. Trefz: *Nucl. Phys.* **A428** (1984) 271
[12] M. Trefz, A. Faessler, W.H. Dickhoff, M. Rhoads-Brown : *Phys. Lett.* **B149** (1984) 459
[13] N. Ohtsuka, M. Shabskiry, R. Linden, M. Müther, A. Faessler: *Nucl. Phys.* **A490** (1988) 715
[14] G. Fäldt, A. Ingemarsson: *Physica Scripta* **28** (1983) 454
[15] P. Roussel et al.: *Phys. Rev. Lett.* **54** (1985) 1779
[16] E.S. Hernandez, S.A. Moszkowski: *Phys. Rev.* **C21** (1980) 929
[17] I. Ahmad: *J. Phys. G (GB)* **4** (1978) 1695 ; I. Ahmad: *J. Phys. G (GB)* **6** (1980) 947
[18] V. Franco, G,K. Varma: *Phys. Rev.* **C18** (1978) 349
[19] D. Slanina, H. McManus: *Nucl. Phys.* **A116** (1968) 271
[20] L.W. Townsend: *Can. J. Phys.* **61** (1983) 93
[21] J. Chauvin, D. Lebrun, A. Lounis, M. Buenerd: *Phys. Rev.* **C28** (1983) 1970
[22] A. Vitturi, F. Zardi: *Phys. Rev.* **C36** (1987) 1404
[23] O.M. Knyazkov, E.F. Hefter: *Z. Phys.* **A301** (1981) 277
[24] F.E. Bertrand et al.: *Phys. Rev.* **C22** (1980) 1832 ; E.E. Gross et al.: *Nucl. Phys.* **A401** (1983) 362
[25] C.W. Dejager, H. Devries, C. Devries: *Atomic data and nuclear data, Tables* **14** (1974) 479
[26] H.B. Bidasaria, L.W. Townsend: *Can. J. Phys.* **61** (1983) 1660
[27] R.G. Stokstad et al.: *Phys. Rev.* **C20** (1979) 655
[28] M. Buenerd et al.: *Nucl. Phys.* **A424** (1984) 313
[29] A. Chaumeaux et al.: *Nucl. Phys.* **A267** (1976) 413
[30] M. Buenerd et al.: *Phys. Rev.* **C26** (1982) 1299
[31] S.M. Lenzi, A. Vitturi, F. Zardi: *Phys. Rev.* **C40** (1989) 2114
[32] S.M. Lenzi, A. Vitturi, F. Zardi: *Phys. Rev.* **C38** (1988) 2086
[33] Love and Franey: *Phys. Rev.* **C24** (1981) 1073
[34] L. Ray: *Phys. Rev.* **C21** (1979) 1857
[35] G. Alberi, L. Bertocchi, G. Bialkowski: *Nuovo Cimento* **3** (1970) 108
[36] A. Ingemarsson, O. Jonsson: *Nucl. Phys.* **A388** (1982) 644
[37] C. Perrin et al.: *Phys. Rev. Lett.* **549** (1982) 1905
[38] D. Aksinenko et al.: *Nucl. Phys.* **A348** (1980) 518